Journal of Magnetic Resonance **145,** 319–325 (2000)
doi:10.1006/jmre.2000.2099, available online at http://www.idealibrary.com on IDEAL®

ENDOR Spectroscopic and Molecular Orbital Study of the Dynamical Properties of the Side Chain in Radical Anions of Ubiquinones Q-1, Q-2, Q-6, and Q-10

Pekka Lehtovuori[1] and Heikki Joela

Department of Chemistry, University of Jyväskylä, P.O. Box 35, FIN-40351 Jyväskylä, Finland

Received December 27, 1999; revised April 7, 2000

The dynamics of the side chain of the radical anions of ubiquinones Q-1 (2,3-dimethoxy-5-methyl-6-[3-methyl-2-butenyl]-1,4-benzoquinone), Q-2, Q-6, and Q-10 have been investigated using electron nuclear double-resonance (ENDOR) spectroscopy. When radicals are produced in the liquid phase, secondary radicals are also formed. The EPR spectra of these additional radicals overlap with the radical of interest. ENDOR spectroscopy was found to be capable for studying the dynamical properties of such conditions. The temperature dependence of the isotropic hyperfine coupling constants of the β- and γ-protons of the side chain was measured. The activation energy of the rotation and other dynamical properties of the side chain were calculated assuming that rotation can be modeled by the classical two-jump model. The rotation energy barrier for Q-1 was also determined by the hybrid Hartree–Fock/density functional method UB3LYP with the 6-31G(d) basis set. Calculated results were in good agreement with the experimental results. Despite the numerous parameters affecting the ENDOR linewidth ENDOR spectroscopy was shown to be a potential method for studying the dynamical properties of the mixtures of the radicals. Prominent forbidden transitions appear in the ENDOR spectra when alkali ions are present in the sample. From these transitions measured ENDOR-induced EPR spectra showed an additional doublet and phase transition in electron Zeeman frequency.

Key Words: **ENDOR; EIE; ubiquinone; dynamic; hindered rotation.**

1. INTRODUCTION

Ubiquinones are found in nature from plant and animal tissues as well as from bacteria with 6 to 10 isoprene subunits in its side chain (Fig. 1). Ubiquinones are known by different names, the most commonly used being ubiquinone-*n*, UQ-*n*, coenzyme Q_n, CoQ_n, and Q-*n*, which is used in this work. The number of isoprene units is indicated by the *n* varying from 1 to 10.

In photosynthesis, ubiquinones have an essential role in the reaction center (RC) where electromagnetic energy is converted to chemical energy. The role and the electronic structure of the quinones in the RC of *Rhodobacteria sphaeroides* have been widely studied (*1–3*) and the behavior of Q_A and Q_B (primary and secondary quinone acceptors, Q-10) is well known. According Stowell *et al.* (*3*) light induces significant changes in Q_B: the quinonic ring rotates 180° around the isoprenic side chain. It is obvious that the ubiquinone's side chain plays an important role in photosynthesis. In this work we clarify some of the dynamical properties of this side chain.

As far as we know, in biological systems there exist only ubiquinones having 6–10 isoprene units. One of the interests of this study is to explore how well Q-1 (2,3-dimethoxy-5-methyl-6-[3-methyl-2-butenyl]-1,4-benzoquinone) can be used as a model compound for larger Q-*n*. This molecule is small enough to carry theoretical calculations with a good basis set in reasonable time. Because suitable data have not been available, the complete electron magnetic resonance (EMR) spectroscopic study of the short side chain ubiquinones Q-1 and Q-2 has been performed.

In earlier studies, a considerable dynamical effect was noticed in electron paramagnetic resonance (EPR) and electron nuclear double-resonance (ENDOR) spectra of Q-10, which is due to hindered rotation of the side chain (*4–6*). However, when decylubiquinone, whose side chain is saturated, was used as a model compound for Q-2, a similar effect was not noticed (*6*).

Dynamical studies of the side chain rotation of the different ubiquinones can be carried out by studying EMR spectra of the corresponding radicals. The isotropic hyperfine coupling (ihfc) of the β-protons of the side chain indicates whether or not the side chain is rotating. This rotation can usually be measured by EPR spectroscopy but because in all measured spectra a secondary radical overlaps with the primary one (*6*), we clarified the capability of ENDOR spectroscopy for solving this kind of problem.

Using ENDOR spectroscopy, ihfc's of primary and secondary radicals can be separated by varying the pumping frequency. Another possibility for separating the spectrum from unwanted species is to use ENDOR-induced EPR (EIE) (*7*) or

[1] To whom correspondence should be addressed. E-mail: pekka@epr.chem.jyu.fi.

1090-7807/00 $35.00

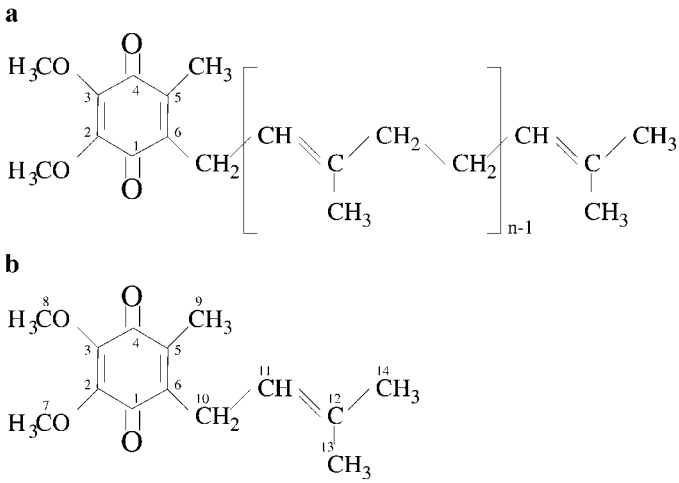

FIG. 1. (a) Molecular structure and IUPAC numbering of Q-*n* and (b) numbering of the carbon atoms in Q-1.

electron nuclear nuclear triple-resonance (TRIPLE)-induced EPR (TIE) spectroscopy. Dynamical studies are not usually carried out by ENDOR spectroscopy because of the number of variables affecting the ENDOR linewidth, the most important being the concentration of the sample and the radio field (rf) modulation amplitude, as well as the power of the microwave (mw) and the rf frequencies. Theory of the linewidths and linewidth alternation in EPR and ENDOR spectroscopy is well known and it is formulated using Bloch equations or relaxation matrix theory (*11–14*).

Earlier, under suitable conditions additional broad lines have been found on the ENDOR spectra of the radical anion of aurins, cyclopolysilanes, and duroquinone (*8–10*). These features have been classified as EPR type background signals or artifacts and are usually found on the low rf-field values complicating the determination of the ^{13}C and ^{2}H couplings. Apparently these features are forbidden transitions and the EIE spectrum measured from such transitions will give good *S*/*N* ratio and increased sensitivity but are more difficult to analyze.

Density functional (DFT) calculations have been carried out for Q-1 and various model compounds (*15*, *16*). However, these calculations have been done mainly without the side chain and therefore the effect of its orientation on the ihfc's and energies of the radical anion of Q-1 is presented here.

2. RESULTS

Dynamical Properties

ENDOR spectra of the ubiquinones Q-*n* showed a remarkable temperature-dependent alternating linewidth effect due to the relative rotation of a side chain and an aromatic ring. Above the coalescence point the ENDOR lines of the β-protons average to one narrow line. Lowering the temperature causes the line to broaden and finally at the coalescence point, it separates into two different ihfc's as shown in Fig. 2.

At temperatures above the coalescence point, the ihfc's vary very little between different ubiquinones: from 0.28 (Q-2) to 0.31 (Q-10), from 2.80 (Q-1) to 2.85 (Q-2), and from 5.77

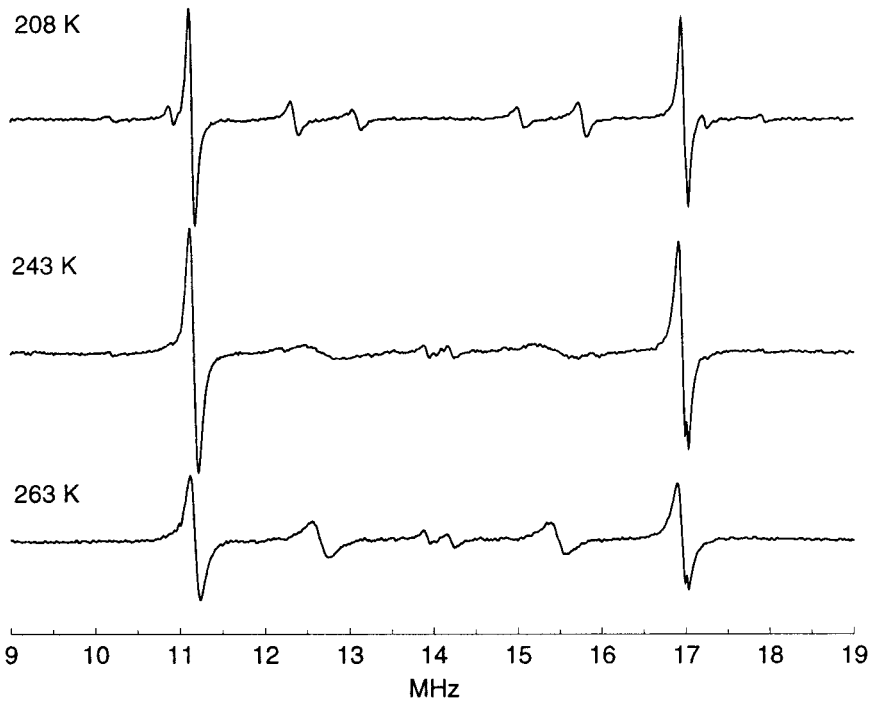

FIG. 2. ENDOR spectra of the radical anion of Q-2 below the coalescence point at 208 K, near the coalescence point at 243 K, and above the coalescence point at 263 K.

TABLE 1
Experimental Spectral Parameters and Coalescence Point Temperatures for Q-1, Q-2, Q-6, and Q-10 in Ethanol

			Groups at carbon[a]			
	T[K]	T_{coal} [K]	6/β-	6/γ-	2,3	5
Q-1		218				
	188		2.110, 3.148			5.781
	263		2.798	0.293		5.779
Q-2		239				
	208		1.943, 3.426			5.846
	263		2.851	0.284	0.076	5.794
Q-6		249				
	208		1.989, 3.404			5.855
	263		2.842	0.294		5.788
Q-10		247				
	208		1.996, 3.424			5.849
	263		2.807	0.314		5.772

Note. All ihfc values are in MHz; the conversion factor into mT is 0.03565 mT MHz^{-1}. Measurement temperatures are selected so that β-proton ihfc's are determined well under and above the coalescence point.

[a] Numbering see Fig. 1.

(Q-10) to 5.79 (Q-2) MHz for γ-protons, β-protons, and methyl protons at 263 K, respectively. Lowering the temperature by 58 K did not have an effect on the methyl group ihfc. However, the effect on the side chain proton ihfc's was remarkable: γ-proton coupling could not be determined and the unequal β-protons resulted in two couplings. The overall spin density in the β-position increases with the length of the side chain. The measured ihfc's are given in Table 1.

If the side chain rotation is described by a two-jump model, the methylene proton ENDOR line broadens in the fast exchange region ($k \gg 2\pi\delta\nu_0$) by (*17*)

$$\Delta\nu = \Delta\nu_0 - \frac{\pi}{2}\,\delta\nu_0^2\tau, \qquad [1]$$

where $\Delta\nu_0$ is the full width at half-height (fwhh) of the unsaturated line in the absence of the exchange and $\delta\nu_0$ is the difference of the two resonance frequencies. The mean lifetime τ is the reciprocal of the chemical rate constant k. In Fig. 3 are shown Arrhenius plots ln(k) vs $1/T$ from which the activation energy E_a and frequency factor can be determined. The results are collected in Table 2.

The mean lifetime at the coalescence point, τ_{coal}, is obtained from (*17*)

$$\tau_{coal} = \frac{\sqrt{2}}{\pi\delta\nu_0}. \qquad [2]$$

Using Eq. [2] the coalescence point temperatures T_{coal} (Table 1) for different Q-n are obtained from the Arrhenius plots. T_{coal}

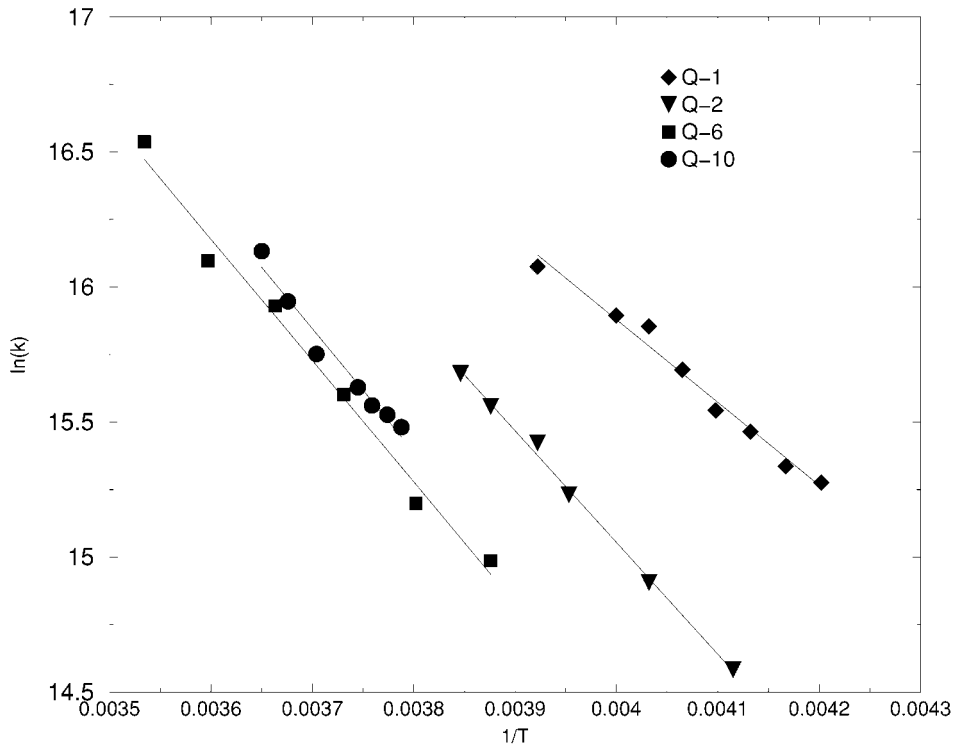

FIG. 3. Arrhenius plots of the side chain rotation of the radical anion of Q-1, Q-2, Q-6, and Q-10 in ethanol.

TABLE 2
Activation Energies E_a, Frequency Factors, and Rate Constants k for Q-1, Q-2, Q-6, and Q-10

	Frequency factor	k^a [1/s]	E_a [kJ/mol]
Q-1	$0.9–1.8 \times 10^{12}$	$5.1–6.3 \times 10^{7}$	26 ± 2
Q-1[b]			28.8
Q-2	$3.3–8.5 \times 10^{13}$	$4.2–4.6 \times 10^{7}$	34 ± 1
Q-6	$0.4–3.2 \times 10^{14}$	$2.8–3.5 \times 10^{7}$	37 ± 2
Q-10	$0.4–6.4 \times 10^{14}$	$3.3–4.1 \times 10^{7}$	38 ± 4
Q-10[c]	$0.1–1.2 \times 10^{13}$		23 ± 3

[a] Calculated at 298 K.
[b] UB3LYP/6-31G(d) calculated.
[c] Das *et al.* (*4*).

depends on the length of the side chain and varies from 218 K (Q-1) to 249 K (Q-10).

Ubiquinone Q-1, as well as Q-2 and Q-6, showed temperature-dependent line broadening and unequalization of ihfc's of β-protons similar to those for Q-10. Therefore it is obvious that hindering of the side chain rotation is due to the rigid structure of the isoprenic group rather than the length of the side chain as it can be assumed on the grounds of the results of decylubiquinone (*6*).

During broadening, the ENDOR lineshape deviates so much from pure Lorentzian that the peak-to-peak linewidths cannot be straightforwardly scaled (scaling factor $\sqrt{3}$) to the fwhh values. Therefore all the ENDOR spectra must be integrated so that linewidths can be determined directly as fwhh from the absorption spectra.

Because Heisenberg exchange broadens lines, the sample was made as dilute as is reasonable, the Q-*n* concentration being $\approx$1 mM. In a too concentrated sample, activation energies can easily be determined as two times too large. Also the effect of rf modulation and mw power was minimized. With the optimal sample, the ENDOR spectrum could be measured at 3 mW of mw power and its effect on the linewidth was insignificant. rf power has a larger effect and the measured linewidths have to extrapolate to zero watts (squared linewidth vs rf power).

When the experiment with Q-10 was repeated in a more viscous solvent, 1-heptanol, the EPR spectrum showed a rate constant of the same order of magnitude at room temperature as in ethanol at 250 K.

Additional Features in ENDOR

At temperatures below 250 K, new couplings were detected in the proton ENDOR spectrum. The couplings can be measured from any of the EPR lines and below the coalescence point they became clearly observable. For Q-1 at 250 K the values are 6.29 and 7.95 MHz and corresponding ihfc's can be detected also from other ubiquinones (Fig. 2). The intensity of these hydrogen couplings in ENDOR is very small but we managed to measure the EIE spectrum of the new radical via the broad peaks which can be interpreted as the forbidden transitions. In the inset in Fig. 4 the outermost part of the EPR spectrum of the radical anion of Q-1 (spectrum b) is shown. The arrow in the inset shows the small peak, probably due to a natural abundance ^{13}C coupling, on the outside of the primary proton EPR spectrum. The ENDOR spectrum (a) was recorded from that point. The arrows in the ENDOR spectrum indicate the rf frequencies from which the EIE spectra (d) and (e) are measured. The third EIE spectrum (c) is measured from the top of the hydrogen coupling at 11.14 MHz. It is in absorption mode and belongs to the radical anion of Q-1. Two other EIE, measured from the top of the broad lines at 2.5 and 8.25 MHz, are like first-derivative spectra with phase shift at electron Zeeman frequency. Additionally, the shape of the EIE spectra is similar to the main radical plus an additional doublet of order of the pumping frequency.

All EIE spectra from proton peaks were observed in absorption mode but the spectra measured from the broad, low rf-field, peaks looked more like derivative spectra. We found that using EIE it was possible to improve sensitivity remarkably.

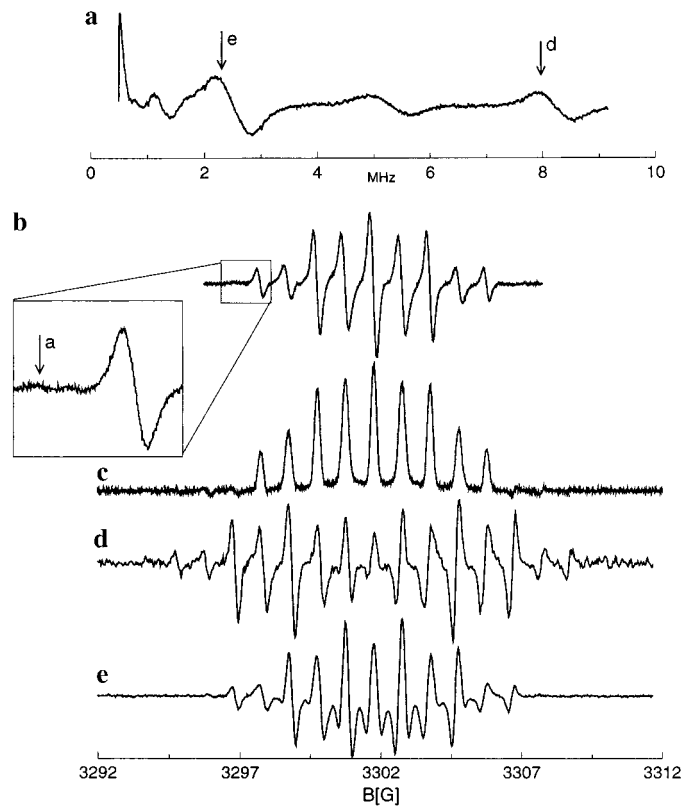

FIG. 4. (a) ENDOR spectrum of Q-1 measured at the small peak indicated by the arrow in a close-up, (b) EPR spectrum, (c) EIE spectrum of Q-1 from the top of the ENDOR peak at 11.14 MHz and the EIEs of the additional radicals measured at different ENDOR peaks, (d) 8.25 MHz, and (e) 2.50 MHz. All spectra are measured at 250 K.

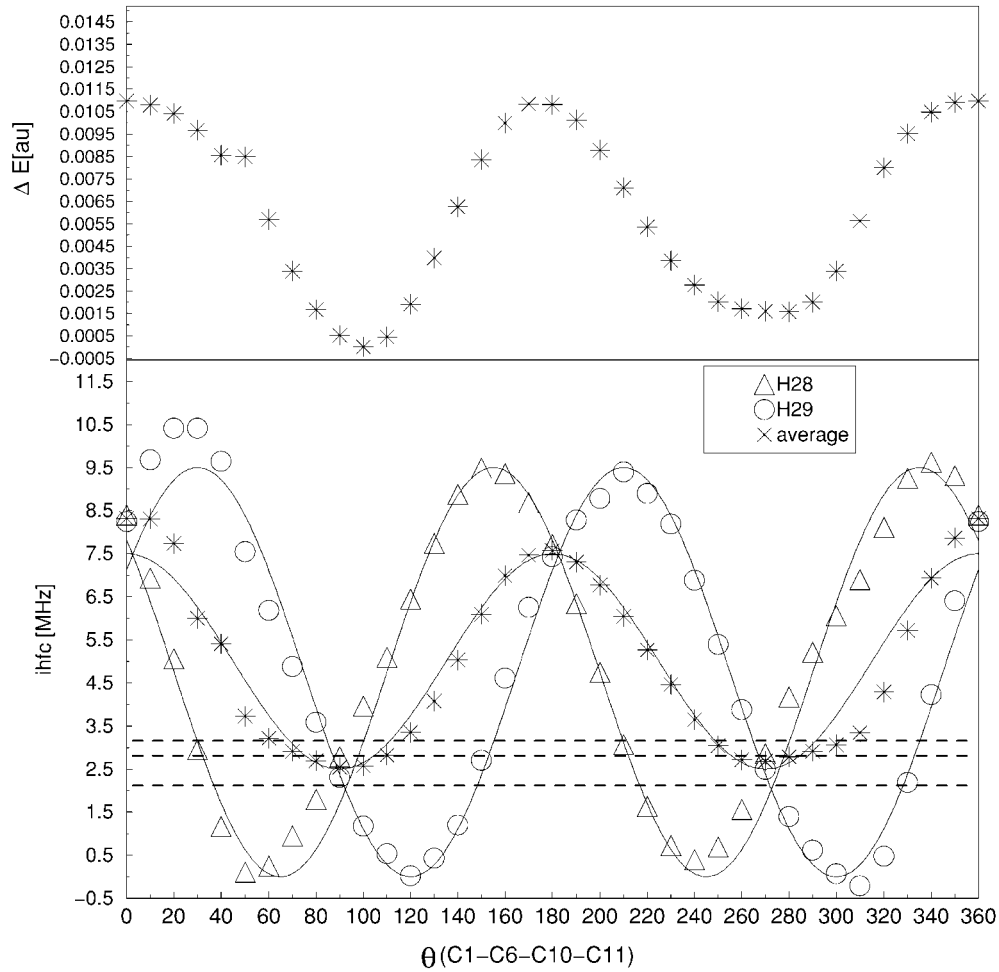

FIG. 5. (Top) UB3LYP/6-31G(d)-calculated rotation energy barrier for radical anion of Q-1. (Bottom) Calculated ihfc's of the two β-protons in different torsion angles C1–C6–C10–C11. The values follow nicely the cosine dependence of Eq. [3]. The dashed horizontal lines indicates the experimental couplings in the slow (2.11 and 3.15 MHz) and fast exchange region (2.80 MHz).

Density Functional Calculations

All DFT calculations were carried out for the Q-1 radical anion. The rotation energy barrier (Fig. 5), calculated as described under Experimental, was 28.8 kJ/mol. It decreased by 0.5 kJ/mol when only the methyl group was kept constrained. The spin density on the side chain varied during side chain rotation. The ihfc's of the β-protons varied from 2.572 to 8.321 MHz. The average values of the calculated ihfc's for the radical anion of Q-1 at selected torsion angles (C1–C6–C10–C11) are given in Table 3. The calculated ihfc values corresponding to the minimum energy conformation ($\theta = 100°$) are in good agreement with the experimental values. Also the individual ihfc's of the β-protons are near the values measured in a slow exchange region. Two separate β-proton couplings can be found on Fig. 5 near the torsion angle of 100°.

The calculated ihfc's of the β-protons follow also quite nicely the well-known cosine dependence

$$a_\beta(\theta) = A + B\cos^2(\theta). \qquad [3]$$

In Fig. 5 the solid lines for the single protons are calculated by Eq. [3] with $A = 0$ MHz and $B = 9.5$ MHz. The average value curve is calculated with $A = 2.5$ MHz and $B = 5$ MHz.

3. DISCUSSION

The measured ihfc's of different ubiquinones are very similar. This is also expected as the unpaired electron is mainly located to quinonic oxygens and the carbon ring. In ENDOR the small γ-coupling can be detected only with certain concentrations and temperatures, and with very low mw power. The spin densities at the side chain farther away from the quinonic ring are small compared to the β- and γ-protons. According to the density functional calculations the spin density is of the same order as the γ-coupling in the methyl groups of the side chain. However, these couplings could not be found from the EPR spectrum. The most remarkable distinction between Q-1 and the other Q-*n* is in the difference of the separated β-couplings. For Q-1 it is near 1.0 MHz and for all other Q-*n* it is

TABLE 3
UB3LYP/6-31G(d)-Calculated ihfc Values for Hydrogens in Q-1 on Different Torsion Angles θ (C1–C6–C10–C11)

	Average values of hydrogen ihfc's [MHz] at different θ[a]					
Position[b]	0	80	100	160	240	320
7 ($-OCH_3$)	−0.095	−0.034	−0.061	−0.118	−0.082	−0.082
8 ($-OCH_3$)	−0.027	−0.039	−0.028	−0.016	−0.045	−0.012
9 ($-CH_3$)	6.357	5.948	6.017	5.911	6.325	5.641
10 (β-)	8.321	2.695	2.572	6.982	3.645	4.291
11 (γ-)	−0.219	−0.215	−0.103	−0.183	−0.264	−0.004
13	−0.142	0.653	0.209	−0.042	−0.079	−0.112
14	−0.136	0.164	0.116	−0.079	−0.083	−0.091

Note. In the cases of many protons in same position the average value of ihfc is given.
[a] $\theta = 100°$ corresponds to the minimum energy geometry.
[b] For numbering see Fig. 1.

over 1.4 MHz, although the sum of the β-couplings is same within 0.1 MHz. This reveals the different behavior of the side chain in Q-1. For Q-*n* to behave near the quinonic ring similarly to those involved in biological processes, the side chain should consist of at least two isoprene units.

The activation energies of the rotation confirm the slightly different behavior of the side chain in Q-1 with respect to others. Q-2 behaves notably more like Q-6 and Q-10 than Q-1. It is evident that the properties of the side chain do not depend linearly on the length of the side chain. The most probable reason for this lies with the different folding of the side chains. The activation energy for rotation of the side chain of Q-10 in ethanol measured in this study is 69% higher than that determined by Das *et al.* (*4*) using ENDOR and 23% higher than what they obtained from EPR linewidth analysis.

The calculated rotation energy barrier for Q-1 (28.8 kJ/mol) is in good agreement with the experimental value (26 ± 2 kJ/mol), although one must remember that in these calculations solvent effects and solvent molecules are excluded.

Also the calculated ihfc's are in good agreement with the experimental ihfc's and therefore use of this method and basis set is justified. As we have shown, there are exceptions in the behavior of the side chain of Q-1 in comparison to other Q-*n*. This must be considered when selecting the model compound for the calculations of the larger systems.

Although there are many parameters affecting the ENDOR linewidth, it is possible to carry out dynamical studies by ENDOR spectroscopy. The fact that ENDOR is much more dependent on surroundings than EPR can also give rise to some difficulties, one being the lack of good solvents. Typically, it is possible to get ENDOR spectra at the needed temperature range only in alcohols (ethanol and 2-propanol) and diethers (1,2-dimethoxyethane). Before performing any dynamical experiments with ENDOR one must ensure that the concentration does not affect the linewidth. In too concentrated samples chemical exchange can broaden lines so much that the phenomenon of interest is undetectable. Measured dynamical parameters are in good agreement with those detected with EPR spectroscopy. Whenever conditions are suitable, ENDOR is a good option. One of the greatest advantages of this method is the possibility of detecting properties of a certain radical in mixtures.

In order to explain small absorptions in the extremes of the EPR spectra (arrow a in Fig. 4) of the radical anion of Q-*n* and the influence of this extra radical on the dynamical parameters, the ENDOR spectra were measured. The relative intensity of these two hydrogen couplings of 6.29 and 7.95 MHz is much larger when measured from the small peak of EPR than from any EPR peak of the main radical. However, all the couplings of the main radical are also present. When perdeuterated ethanol (CD_3CD_2OD) was used, these couplings were not detected, indicating some kind of proton adduct to the quinone oxygens. The broad forbidden transitions were however present in the low-field ENDOR, complicating the analysis of deuterium couplings.

The broad lines in low rf field are always reported on more or less similar kinds of radicals and conditions. Earlier these absorptions have been called baseline problems or artifacts (*9*, *10*), but according to our preliminary calculations by *xemr* (*19*) these lines can be simulated as forbidden transitions where the two nuclear spins change simultaneously. By adjusting the experimental conditions it is possible to remove these broad lines completely (*10*). The reason for these forbidden transitions appearing so clearly in some circumstances might lie in the dipolar or quadrupolar influence of the alkali metal counterion. The appearance of the phase shifting in the EIE is probably caused by the superposition of many slightly different frequencies in the broad ENDOR line. Our finding provides a new approach to the study of the radical–ion pairs. The precise study of the broad ENDOR transitions in the aid of computation of the energy states and the complete analysis of the forbidden transitions has begun on the simpler benzoquinone and duroquinone systems.

The structure and the spin distribution of the radicals can be

identified in normal cases, but in studies of the solvent effects and dynamical properties there are considerably more variables. Since the great majority of the reactions occur in the liquid phase, understanding interactions of radicals, ion pairs, and solvent molecules is indispensable. Understanding the broad, "EPR-type" lines in the liquid-state ENDOR spectrum might provide new information on the interactions of radicals in solutions.

4. EXPERIMENTAL

Materials, Equipment, and Sample Preparation

Coenzymes Q-1, Q-2, Q-6, and Q-10 were Sigma products and were used without further purification. 1-Heptanol (>99%) and 40% NaOD in D_2O were from Merck. KOH pellets (86.4%) were from Baker Analyzed. Ethanol for spectroscopic purpose (min. 99.5%) was prepared by Primalco Oy and perdeuterated ethanol (CD_3CD_2OD, HDO + D_2O < 0.3%) by Euriso-top.

Spectra were recorded on a Bruker ER 200 D-SRC spectrometer equipped with a Varian E-12 magnet, Bruker ER 033M FF-lock, and Bruker EN 810 ENDOR unit. The applied microwave power varied for ENDOR measurements from 3 to 10 mW. All spectra were collected and analyzed using the *xemr* program (*19*). The accuracy of the temperature controller was determined to be ± 1 K.

Radical anions were prepared under high-vacuum conditions in alkaline ethanol, CD_3CD_2OD, and 1-heptanol with potassium hydroxide as a reducing agent. KOH was dissolved to solvent and put into the cuvette after which coenzyme Q-*n* was put into the cuvette in the capillar tube. The sample was frozen in liquid nitrogen and connected to the vacuum line (ca. 5×10^{-6} Torr). After repeating freeze–pump–thaw cycles twice, the cuvette was sealed with a flame. Sample concentrations were 1 mM ubiquinone Q-*n* and 0.5 M KOH. Total volume of the sample (130 μl) was under a temperature control.

Density Functional Calculations

All calculations were carried out using the UB3LYP/6-31G(d) DFT method. The UB3LYP method is the spin-unrestricted Becke's three-parameter hybrid Hartree–Fock/density functional method with the Lee–Young–Parr correlation functional (*20–23*). The method is known to work well in calculations of ihfc's and energies of quinone radicals (*25, 26*). Calculations were carried out only for Q-1 because of the large size of the other molecules and numerous local energy minima of the longer side chains. The rotational energy barrier was determined by changing the torsion angle C1–C6–C10–C11 in 10° steps and keeping the ring structure and the methoxy groups constrained. Near the minimum and maximum the entire geometry was optimized, keeping only the methyl group locked so that it hinders the side chain rotation as much as possible. All calculations were carried out using GAUSSIAN 94 (*24*) revision D4 on Silicon Graphics Origin 200 and Indigo 2 computers.

ACKNOWLEDGMENT

Financial support from TEKES is gratefully acknowledged.

REFERENCES

1. R. A. Isaacson, F. Lendzian, E. C. Abresch, W. Lubitz, and G. Feher, *Biophys. J.* **69,** 311 (1995).
2. W. Lubitz and G. Feher, *Appl. Magn. Reson.* **17,** 1 (1999).
3. M. H. B. Stowell, T. M. McPhillips, D. C. Rees, S. M. Soltis, E. Abresch, and G. Feher, *Science* **276,** 812 (1997).
4. M. R. Das, H. D. Connor, D. S. Leniart, and J. H. Freed, *J. Am. Chem. Soc.* **92,** 2258 (1970).
5. G. Feher, R. A. Isaacson, M. Y. Okamura, and W. Lubitz, *in* "Series of Chemical Physics, Vol 42: Antennas and Reaction Centers of Photosynthetic Bacteria, Structure, Interactions and Dynamics" (M. E. Michel-Beyerle, Ed.), p. 42, Springer-Verlag, Berlin/New York (1985).
6. H. Joela, S. Kasa, P. Lehtovuori, and M. Bech, *Acta Chem. Scand.* **51,** 233 (1997).
7. J. S. Hyde, *J. Chem. Phys.* **43,** 1806 (1965).
8. B. Kirste, W. Harrer, and H. Kurreck, *J. Am. Chem. Soc.* **107,** 20 (1985).
9. B. Kirste, R. West, and H. Kurreck, *J. Am. Chem. Soc.* **107,** 3013 (1985).
10. B. Kirste, *J. Magn. Reson.* **62,** 242 (1985).
11. A. Carrington, *Mol. Phys.* **5,** 425 (1962).
12. J. H. Freed and G. K. Fraenkel, *J. Phys. Chem.* **39,** 326 (1963).
13. J. H. Freed and G. K. Fraenkel, *J. Chem. Phys.* **41,** 3623 (1964).
14. D. S. Leniart, H. D. Connor, and J. H. Freed, *J. Chem. Phys.* **63,** 165 (1975).
15. S. E. Boesch and R. A. Wheeler, *J. Phys. Chem.* **101,** 5799 (1997).
16. M. Nonella, *J. Phys. Chem. B* **102,** 4217 (1998).
17. H. Kurreck, B. Kirste, and W. Lubitz, "Electron Nuclear Double Resonance Spectroscopy of Radicals in Solution: Application to Organic and Biological Chemistry," VCH, New York (1988).
18. R. I. Samoilova, N. P. Gritzan, A. J. Hoff, W. B. S. van Liemt, J. Lugtenburg, A. P. Spoyalov, and Y. D. Tsvetkov, *J. Chem. Soc., Perkin Trans. 2,* 2063 (1995).
19. J. Eloranta, *xemr,* ftp://epr.chem.jyu.fi/pub.
20. A. D. Becke, *J. Chem. Phys.* **98,** 5648 (1993).
21. S. H. Vosko, L. Wilk, and M. Nusair, *Can. J. Phys.* **58,** 1200 (1980).
22. C. Lee, W. Yang, and R. G. Parr, *Phys. Rev. B* **37,** 785 (1988).
23. B. Miehlich, A. Savin, H. Stoll, and H. Preuss, *Chem. Phys. Lett.* **157,** 200 (1989).
24. M. J. Frisch, G. W. Trucks, H. B. Schlegel, P. M. W. Gill, B. G. Johnson, M. A. Robb, J. R. Cheeseman, T. Keith, G. A. Petersson, J. A. Montgomery, K. Raghavachari, M. A. Al-Laham, V. G. Zakrzewski, J. V. Ortiz, J. B. Foresman, J. Cioslowski, B. B. Stefanov, A. Nanayakkara, M. Challacombe, C. Y. Peng, P. Y. Ayala, W. Chen, M. W. Wong, J. L. Andres, E. S. Replogle, R. Gomperts, R. L. Martin, D. J. Fox, J. S. Binkley, D. J. Defrees, J. Baker, J. P. Stewart, M. Head-Gordon, C. Gonzalez, and J. A. Pople, Gaussian, Inc., Pittsburgh, PA (1995).
25. J. Eloranta, V. Vatanen, K. Vaskonen, R. Suontamo, and M. Vuolle, *J. Mol. Struct. (THEOCHEM)* **424,** 249 (1998).
26. J. Eloranta, R. Suontamo, and M. Vuolle, *J. Chem. Soc., Faraday Trans.* **93,** 3313 (1997).